JACS
JOURNAL OF THE AMERICAN CHEMICAL SOCIETY
Article
pubs.acs.org/JACS

Preventing Alkyne−Alkyne (i.e., Glaser) Coupling Associated with the ATRP Synthesis of Alkyne-Functional Polymers/Macromonomers and for Alkynes under Click (i.e., CuAAC) Reaction Conditions

Porakrit Leophairatana, Sanjoy Samanta, Chathuranga C. De Silva, and Jeffrey T. Koberstein*

Department of Chemical Engineering, Columbia University, 500 West 120th Street, New York, New York 10027, United States

Supporting Information

ABSTRACT: Alkyne-functional polymers synthesized by ATRP exhibit bimodal molecular weight distributions indicating the occurrence of some undesirable side reaction. By modeling the molecular weight distributions obtained under various reaction conditions, we show that the side reaction is alkyne−alkyne (i.e., Glaser) coupling. Glaser coupling accounts for as much as 20% of the polymer produced, significantly compromising the polymer functionality and undermining the success of subsequent click reactions in which they are used. Glaser coupling does not occur during ATRP but during postpolymerization workup upon first exposure to air. Two strategies are reported that effectively eliminate these coupling reactions without the need for a protecting group for the alkyne-functional initiator: (1) maintaining low temperature post-ATRP upon exposure to air followed by immediate removal of copper catalyst; (2) adding excess reducing agents post-ATRP which prevent the oxidation of Cu(I) catalyst required by the Glaser coupling mechanism. Post-ATRP Glaser coupling was also influenced by the ATRP synthesis ligand used. The order of ligand activity for catalyzing Glaser coupling was: linear bidentate > tridentate > tetradentate. We find that Glaser coupling is not problematic in ARGET-ATRP of alkyne-terminated polymers because a reducing agent is present during polymerization, however the molecular weight distribution is broadened compared to ATRP due to the presence of oxygen. Glaser coupling can also occur for alkynes held under CuAAC reaction conditions but again can be eliminated by adding appropriate reducing agents.

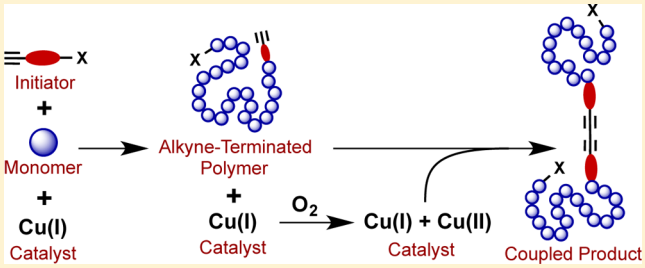

INTRODUCTION

Over the past few decades, "click" chemistry has emerged as a vital and versatile conjugation tool for a wide variety of molecular and macromolecular transformations, with applications in pharmaceuticals,[1−4] chemical synthesis,[5−7] polymer chemistry,[8−13] carbohydrate chemistry,[14,15] sensor/diagnosis,[16−18] and both surface and functional group modifications.[19−23] Although Sharpless and co-workers identified several important reactions that meet the qualifications to be considered as "click" chemistry,[24] Cu(I)-catalyzed alkyne−azide cycloaddition (CuAAC)[25] is considered by many to be the gold standard because of its mild reaction conditions, functional group tolerance, and quantitative yield.

CuAAC reactions have proven especially powerful in polymer synthesis, as a convenient means for the preparation of a wide variety of hierarchically structured macromolecules including linear homopolymers,[26] end-linked gels,[27−29] block copolymers,[30,31] dendrimers,[32] macrocyclic polymers,[33] polymeric catenanes,[34] miktoarm star polymers,[35−37] polymacromomers,[38] and copolymacromers.[38] The success of CuAAC-based supramolecular chemistry relies on the ability to prepare well-characterized building blocks: alkyne-terminated and azide-terminated polymers/macromonomers. Controlled radical polymerization techniques, in particular atom transfer radical polymerization (ATRP),[39] are generally recognized as the most successful means for preparing these click-functional polymers/macromonomers. Alkyne functionality is readily provided by the use of an alkyne-functional initiator, while azide functionality is obtained by a postpolymerization S_N2 reaction of the halide terminus (i.e., chlorine or bromine) with sodium azide.

In practice, however, functional polymers prepared by ATRP are prone to side reactions including radical−radical coupling[34,40,41] of bromine termini and Glaser coupling of alkyne termini,[10,33,41−47] which compromise the macromonomer functionality and their subsequent utility for the synthesis of well-defined, hierarchically structured materials by CuAAC end-linking reactions.

ATRP of an alkyne-terminated polymer is illustrated in Figure 1. The initiator chosen for this purpose is usually an alkyne molecule with secondary or tertiary bromine functionality, the latter of which serves to initiate the controlled radical polymerization reaction. The fact that each initiator molecule contains one alkyne group is generally thought to virtually guarantee that each polymer chain is terminated with alkyne functionality, enabling subsequent CuAAC end-linking reactions. Two undesirable polymer−polymer coupling reactions

Received: December 14, 2016
Published: February 20, 2017

DOI: 10.1021/jacs.6b12525
J. Am. Chem. Soc. 2017, 139, 3756−3766

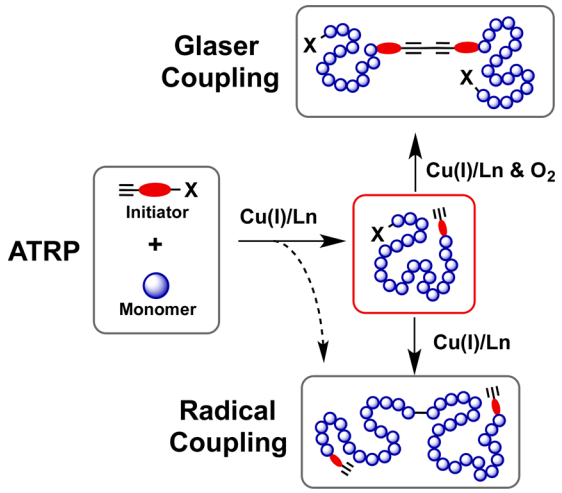

Figure 1. Radical–radical and Glaser coupling reactions during and after ATRP (Ln = N ligand, X = Cl or Br).

can occur, however, that compromise the fidelity of this synthesis and the purity of the resultant polymeric click-functional "building blocks", as shown in the figure. Radical–radical coupling of the growing chain ends produces a dialkyne-terminated telechelic macromonomer, while Glaser coupling of two alkyne termini produces a dibromo-terminated telechelic macromonomer. These "impurities" contaminate the desired product, broaden its molecular weight distribution, and decrease its functionality.

Methods are available to minimize radical–radical coupling,[8] however the elimination of Glaser coupling remains problematic. Glaser coupling of alkynes is a valuable tool in organic synthesis,[48−54] and its widely accepted mechanism is illustrated in Figure 2.[55,56] Both Cu(I) and Cu(II) are required as catalysts

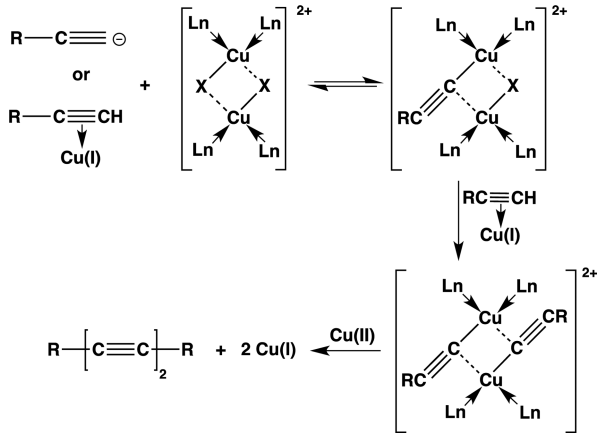

Figure 2. Mechanism of oxidative acetylenic Glaser Coupling proposed by Bohlmann et al.[55] (Ln = N ligand, X = Cl or Br).

along with a ligand. Because ATRP also employs a ligand and uses Cu(I) as a catalyst, experimental conditions that favor the conversion of Cu(I) to Cu(II) can lead to Glaser coupling of the alkyne-terminated polymers produced by ATRP. More recently a modified mechanism for Glaser coupling[57] was proposed based upon density functional theory as shown in Figure 3. This mechanism requires Cu(I) and a nitrogen-based ligand, but does not expressly require Cu(II); instead a Cu(I)/Cu(III)/Cu(II)/Cu(I) catalytic cycle is proposed and oxygen is

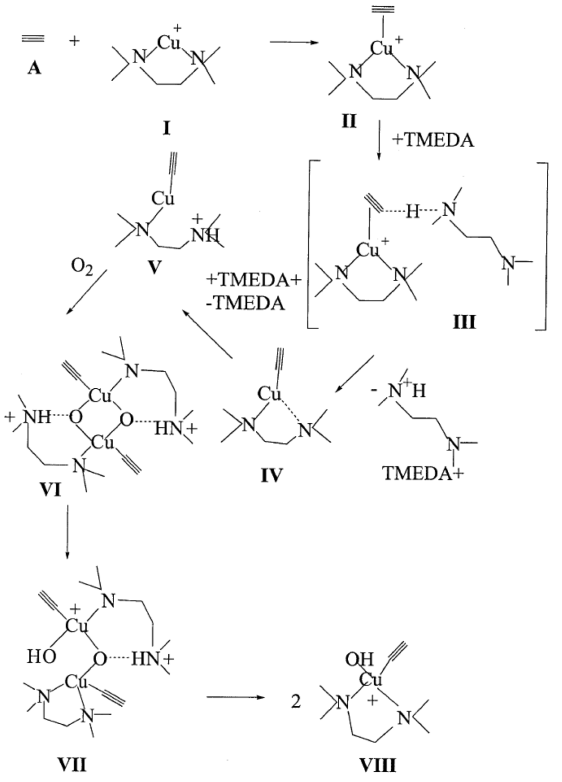

Figure 3. Mechanism of oxidative acetylenic Glaser Coupling proposed by Fomina et al.[57]

required. Compound VIII in Figure 3 eventually dissociates to form the ultimate coupled product, a diacetylene.

Attempts have been made to prevent Glaser coupling during ATRP by using protection/deprotection strategies,[10,30,37,45] such as protection with trimethylsilyl (TMS) or triisopropylsilyl (TIPS) groups followed by deprotection with reagents such as tetrabutylammonium fluoride (TBAF). These strategies have not proven to be universally reliable or effective, however, because protecting groups such as TMS have been found to be labile under a variety of different experimental conditions[30] and because the harsh reagents required to deprotect TIPS can degrade the polymers formed. In the case of TIPS, for example, deprotection can degrade the ester linkage in the propargyl 2-bromoisobutyrate initiator normally used to synthesize alkyne-terminated polymers by ATRP. This degradation can be avoided by replacing the ester linkage by an amide, however at the cost of a broader molecular weight distribution.

Although generally considered to be highly orthogonal, the CuAAC reaction is also subject to certain side reactions.[58,59] In particular, because CuAAC also relies upon copper catalysis, Glaser coupling can occur as illustrated in Figure 4. For example, attempts to couple an alkyne-functional peptide with an azide-functional peptide via liquid phase CuAAC resulted in the formation of 1,3-diyenes as byproducts.[60] Reports have also indicated the occurrence of Glaser coupling side reactions during CuAAC of alkyne-functional small molecules and macromolecules.[61] While there have been some efforts to prevent these side reactions from occurring, for example by using solid phase CuAAC[47] and by adding reducing agents,[62] general methods to eliminate Glaser coupling during ATRP and CuAAC of alkyne-functional materials are still lacking.

In light of these challenges, we report a detailed examination of Glaser coupling side reactions associated with ATRP of

DOI: 10.1021/jacs.6b12525
J. Am. Chem. Soc. 2017, 139, 3756−3766

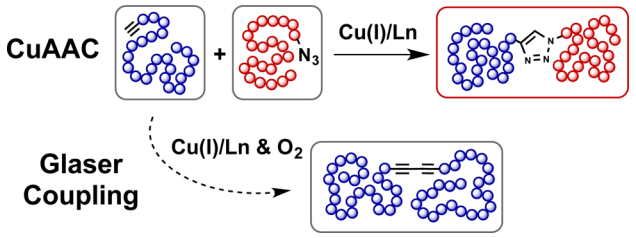

Figure 4. Schematic representation of a CuAAC reaction between alkyne terminated and azide terminated polymers; and undesirable alkyne–alkyne Glaser coupling side reaction (Ln = N ligand).

alkyne-terminated polymers and for alkynes held under CuAAC reaction conditions, and propose two new strategies for their elimination. We also show that careful choice of a nitrogen-based ligand can significantly reduce but not eliminate Glaser coupling reactions associated with the ATRP synthesis of alkyne-terminated polymers.

RESULTS AND DISCUSSION

Glaser Coupling, a Side Reaction to ATRP. The GPC trace for a typical alkyne end-functional polymer synthesized by ATRP, α-alkyne,ω-Br-PS, is shown in Figure 5. There is a main

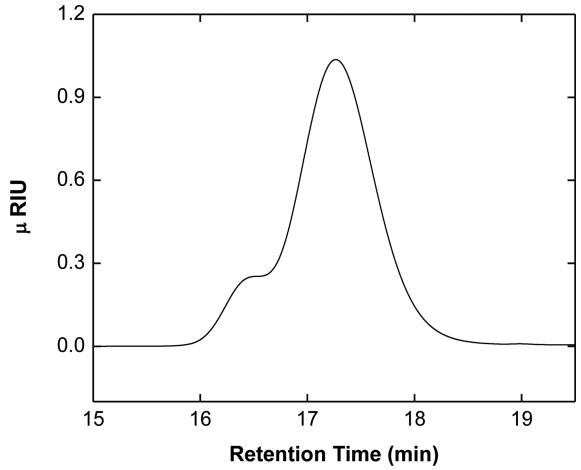

Figure 5. Typical GPC trace of alkyne end-functional polymer synthesized by ATRP.

peak centered at the target molecular weight for the synthesis, and a satellite shoulder/peak at lower elution volume indicating the presence of an undesirable polymer with molecular weight greater than the target molecular weight.

The most likely origin of the undesirable byproduct is the formation of coupled product by an end-linking reaction to yield a polymer with precisely twice the target molecular weight. If the byproduct is the result of an end-linking or coupling reaction, then its molecular weight distribution can be calculated by self-convolution of the molecular weight distribution of the uncoupled polymer (see eq 1). Figure 6 illustrates that the bimodal molecular weight distribution of end-functional polymer produced by ATRP can be quantitatively reproduced by assuming that the undesirable byproduct is the result of a polymer coupling reaction. Although the shoulder apparent in the molecular weight distribution shown in Figure 5 might often be dismissed as a negligible fraction of the total molecular weight, the modeling for the case shown indicates that end-coupled polymer accounts for about 20% by

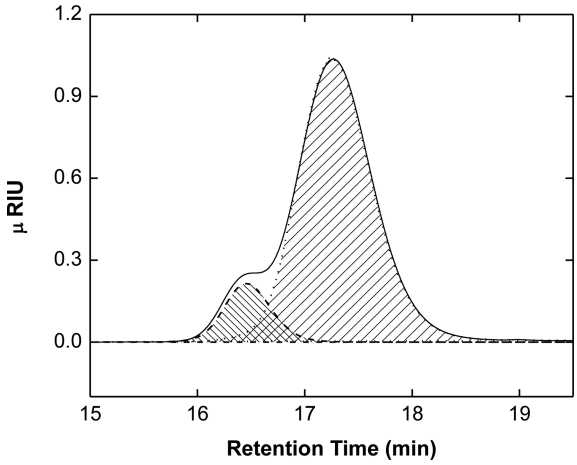

Figure 6. Best fit (simulated by self-convolution) normalized GPC signals of alkyne end-functional polymer (dotted line) and coupled polymer (dashed line).

weight of the total polymer product, significantly reducing its functionality and compromising its utility in producing well-defined supramolecular structures by subsequent CuAAC reactions.

Alkyne-functional polymers prepared by ATRP have one alkyne-functional chain end provided by the initiator, and one bromine atom at the active chain end where monomer addition occurs. There are therefore two possible side reactions to account for polymer coupling or end-linking: acetylenic coupling between two terminal alkyne groups or radical–radical coupling between two polymeric alkyl bromides as shown in Figure 1. These coupling reactions are undesirable as they decrease the ultimate alkyne/click functionality and increase the polydispersity index (PDI), compromising the precise control over polymer properties that is normally offered by ATRP. The loss of functionality is of particular importance as these functional polymers are macromonomers used to produce a variety of hierarchically structured macromolecules of varying architecture and increased complexity. The loss of control over macromonomer functionality and structure leads to defects in the complex supramolecular materials they are intended to produce.

The question of which of the two end-linking reactions is responsible for the coupled byproduct may be answered in part by performing ATRP using a nonfunctional initiator, in which case only radical–radical coupling is possible. For this purpose, nonfunctional PS was synthesized with the nonfunctional bromine initiator (EBiB) using CuBr/dNbpy as the catalyst-ligand complex. Immediately after polymerization, the GPC trace in Figure 7 (solid line), indicates a monodisperse product without any indication of coupling. Even after exposure to air for 18 h (the open circles in Figure 7) there is no indication of polymer coupling. Similarly, Figure S.1 in the Supporting Information shows no coupling for nonfunctional PS at higher molecular weight (Mn $\approx$ 10 000 g·mol^{-1}) after exposure to air. One can reasonably conclude therefore that the polymer byproduct evidenced in Figure 5 is not the result of radical–radical coupling.

To corroborate this conclusion, we used ^{1}H NMR to study coupling in the small molecule alkyne-functional initiator itself in the presence of various ATRP catalysts and ligands. For this purpose, PgBiB was incubated with CuBr and PMDETA in THF and then exposed to air for 24 h. Figure 8 shows the ^{1}H

DOI: 10.1021/jacs.6b12525
J. Am. Chem. Soc. 2017, 139, 3756–3766

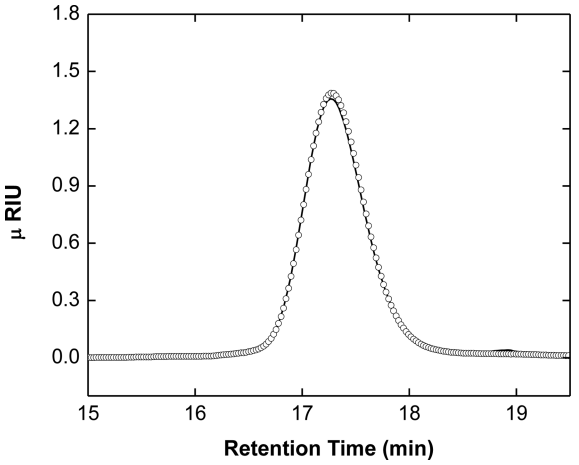

Figure 7. Superimposed GPC chromatograms of nonfunctional PS (2840 g·mol^{-1}; 1.11). Solid black line: taken immediately after completion of the ATRP. Open circle (plotted for every 30th data points): taken after 18 h of exposure to air.

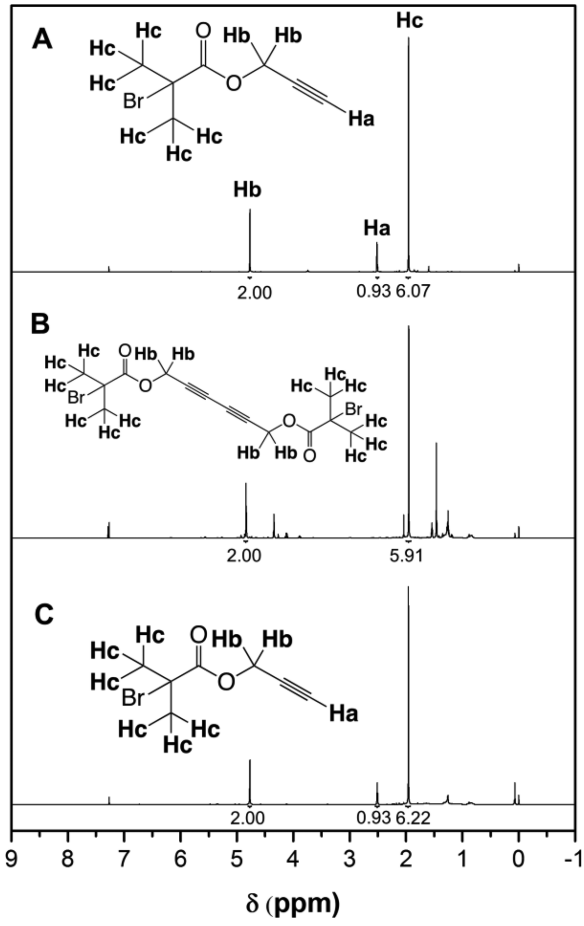

Figure 8. (A) ^{1}H NMR (400 MHz) spectra for PgBiB in $CDCl_3$. ^{1}H NMR spectra of a 24-h incubation of PgBiB with (B) CuBr and PMDETA in THF and (C) $CuBr_2$ and PMDETA in THF.

NMR spectra of pure PgBiB initiator, before (Figure 8A) and after 24-h incubation in air (Figure 8B). The spectra show a minute reduction in the ^{1}H NMR relative peak area at δ = 1.96 ppm from 6.07 to 5.91, indicating minimal radical−radical coupling and a clear disappearance of the acetylene peak at δ = 2.51 ppm, suggesting that the preponderance of coupling for the pure alkyne-functional ATRP initiator in the presence of air can be attributed to acetylenic Glaser coupling and is not associated with radical−radical coupling.

On the basis of the Bohlmann et al.[55] mechanism for Glaser coupling, it is unlikely that acetylenic coupling can occur during ATRP. Glaser coupling requires both Cu(I) and Cu(II) as catalysts. ATRP, however, uses only Cu(I) as a catalyst and is carried out in the absence of oxygen so that there is little likelihood for formation of Cu(II) by oxidation of Cu(I) under ATRP reaction conditions. It is reasonable to expect therefore that Glaser coupling occurs postpolymerization when the ATRP reactor is opened and the synthesis products are first exposed to air.

Figures 9 and 10 show that upon exposure to air, Cu(I) is oxidized to Cu(II), forming the catalysts required for Glaser

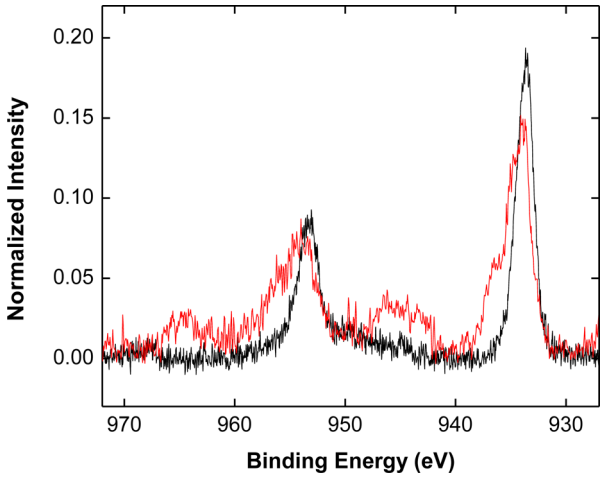

Figure 9. XPS spectra of Cu(I)Br/dNbpy (black line) and Cu(II)Br_2/dNbpy thin films (red line).

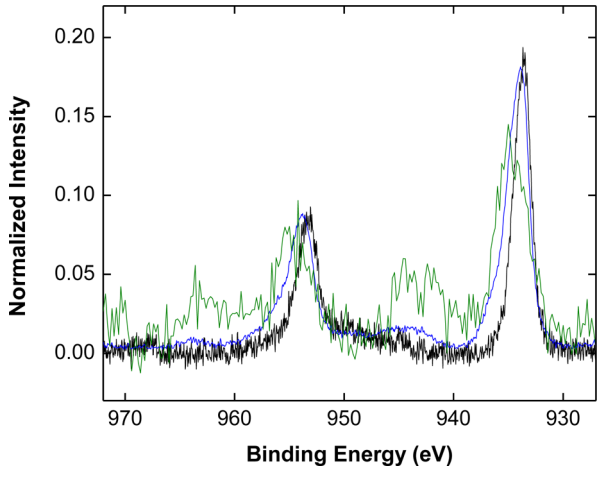

Figure 10. XPS spectra of Cu(I)Br/dNbpy thin films before oxidation (black line) and after a 24-h exposure to air (green and blue lines) indicating conversion of Cu(I) to Cu(II). Collection times (cycles): 1 (green), 50 (blue), and 10 (black).

Coupling. ATRP of styrene was performed using CuBr/dNbpy catalyst complex and after 70 min, a sample was collected and dried under anaerobic conditions. The thin film on a silicon wafer was subsequently analyzed via XPS showing Cu $2p_{3/2}$ and Cu $2p_{1/2}$ peaks at 933 and 953 eV, respectively (black lines in Figures 9 and 10). Cu(II)Br_2/dNbpy in styrene was also dry

DOI: 10.1021/jacs.6b12525
J. Am. Chem. Soc. 2017, 139, 3756−3766

casted into a thin film and subsequently analyzed via XPS (Figure 9, red line) showing a shift of the Cu $2p_{3/2}$ peak toward 935 eV and the presence of a series of satellites at 943, 945, and 964 eV. The remaining ATRP solution was exposed to air and after 24 h, the solution was dry casted into a thin film and analyzed via XPS as shown in Figure 10 (blue and green spectra).

The shift of Cu $2p_{3/2}$ toward higher binding energy and the appearance of the satellites confirm that Cu(II) was generated upon exposure to air.

The strength of the copper XPS signals are lower than ideal due to several factors: (i) copper is present in only catalytic amounts; (ii) due to surface reorganization, copper is always buried beneath organic material thus attenuating its signal; and (iii) data collection time was minimized because prolonged exposure to the X-ray beam under high vacuum may alter the sample due to the reduction of Cu(II) to Cu(I) or Cu(0); indicated by the decrease in the satellite peaks after 50 cycles of XPS data collection (blue line) compared to that from 1 XPS cycle (green line). Despite the experimental challenges, the data in Figures 9 and 10 clearly show that Cu(II) forms post-ATRP upon exposure to air.

The hypothesis that Glaser coupling occurs postpolymerization was validated by performing GPC analysis of molecular weight distributions as a function of time exposed to air following polymerization. The results are shown in Figure 11,

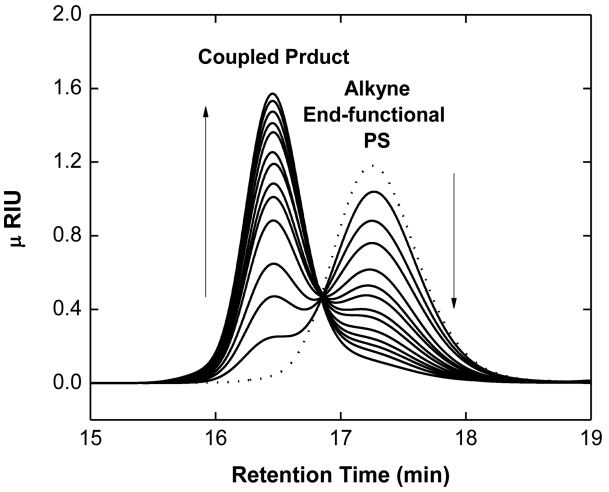

Figure 11. GPC spectra for α-alkyne,ω-Br-PS (····Mn = 2930 g·mol^{-1}, PDI = 1.09) and coupled products taken as a function of time after exposure to air at room temperature.

for α-alkyne,ω-Br-PS for the first 20 h of exposure to air after ATRP. Initially, the product is composed primarily of the target product with a molecular weight fraction centered at an elution time of 17.4 min. Upon exposure to air, the fraction of coupled byproduct (observed at 16.4 min) increases steadily with time. Figure S.2 also shows the same trend for α-alkyne,ω-Br-P*t*BA after exposure to air, as indicated by a gradual decrease in the target product peak and a simultaneous increase in the coupled product peak. From these results, it can be concluded that the preponderance of coupled product observed in alkyne-terminated polymers prepared by ATRP is associated with Glaser coupling that occurs postpolymerization upon exposure to air.

The conclusion that coupling occurs post-ATRP upon exposure to air is consistent with both Glaser coupling mechanisms. In the case of the Bohlmann et al.[55] mechanism (Figure 2), oxidization of the Cu(I) ATRP catalyst provides both the Cu(I) and Cu(II) catalysts required. In the case of the Fomina et al.[57] mechanism (Figure 3), exposure to air supplies the required oxygen and enables the Cu(I)/Cu(III)/Cu(II)/Cu(I) catalytic cycle.

The kinetics of the Glaser coupling reaction can be followed by analysis of the GPC data with a model that describes how end-linking alters the molecular weight distribution. The molecular weight distribution of the coupled product can be calculated by taking the self-convolution of the molecular weight distribution of uncoupled polymer[63] following eq 1, where N is the molar fraction of the coupled chains with degree of polymerization of Z and N_1 and N_2 are the molar fraction of chains of the first and second polymer with length i and $Z - i$, respectively.

$$N(Z) = \sum_{i=Z-1}^{i=1} N_1(i)N_2(Z-i) \quad (1)$$

Using this approach, the extent of polymer coupling as a function of exposure time to air can be determined by fitting the GPC traces, as shown in Figure 12. The peak of the alkyne-

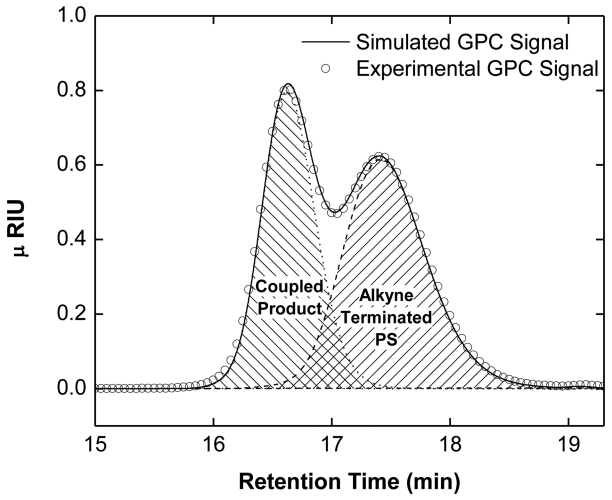

Figure 12. Experimental GPC signal plotted for every 30th data point of α-alkyne,ω-Br-PS after 30 min of Glaser Coupling (○). Simulated GPC signal (—), where the dashed line is the contribution from uncoupled alkyne polymer, and the dotted line is the contribution from coupled product.

terminated polymer was first characterized by GPC immediately after the ATRP reaction with minimal exposure to air to prevent Glaser coupling from occurring as represented by the dashed lines in Figure 12. By applying a quartic polynomial fit to the GPC calibration of polystyrene standards, the raw GPC signal was first converted to a weight distribution and subsequently to a number distribution. The mathematical self-convolution was then performed to simulate the distribution of the coupled product (Figure 12, dotted line) assuming equal reactivity among each chain length of the polymer.

Finally, the fractions of coupled and uncoupled polymers were determined by minimizing the sum of squared errors between the simulated and experimental GPC traces. Knowledge of the fraction of coupled and uncoupled products allows the conversion to be calculated as a function of exposure time to air postpolymerization.

DOI: 10.1021/jacs.6b12525
J. Am. Chem. Soc. 2017, 139, 3756−3766

Figure 13 shows the conversion of the Glaser coupling reaction as a function of the exposure time to air post-ATRP.

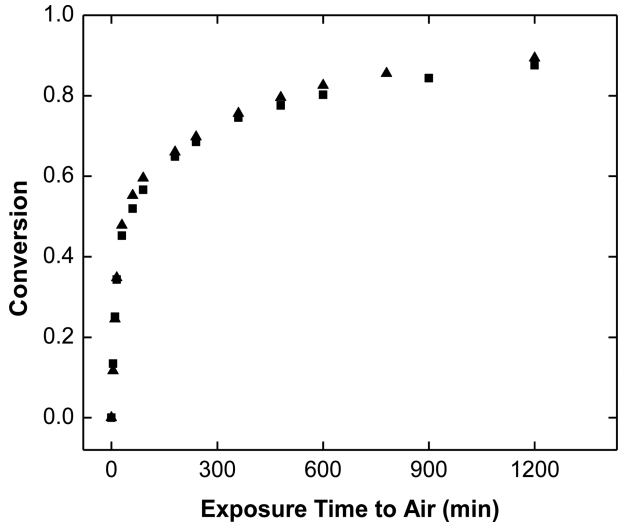

Figure 13. Conversion of the Glaser coupling reaction for α-alkyne,ω-Br-PS (▲ Mn = 2930 g·mol^{-1}, PDI = 1.09, and ■ Mn = 3,180 g·mol^{-1}, PDI = 1.09) as a function of exposure time to air postpolymerization.

On the basis of the bimolecular mechanism for Glaser coupling, the rate is expected to be second order in the alkyne concentration. However, several factors are expected to complicate the post-ATRP polymer−polymer coupling reaction and lead to reaction kinetics that are not second order. For example, it is expected that initially, macroscopic diffusion of oxygen and the rates of Cu(II) generation would control the rate of the coupling reaction. Once the concentration of oxygen reaches equilibrium at saturation and a catalytic amount of Cu(II) has formed, the anticipated second-order Glaser coupling kinetics may still not be relevant as the coupling reaction may be controlled by diffusion of the alkyne-functional polymers/macromonomers, which will depend on polymer concentration, chain length, and solvent quality.[64] Finally, as the concentration of Cu(I) diminishes, the rate may depend on the concentrations of Cu(I) in the solution and the stability of the Cu(I)/ligand complex.

The kinetics of Glaser coupling for α-alkyne,ω-Br-PS were also followed by ^{1}H NMR as shown in Figure 14 (full ^{1}H NMR spectra shown in Figure S.3). The reaction conditions were identical to those of the previous Glaser coupling kinetic experiments; however, in this case, perdeuterated styrene (98% deuterated) monomer was used for the ATRP synthesis so that the majority of the protons in the α-alkyne,ω-Br-PS were associated with the initiator fragment. The occurrence of Glaser coupling was therefore indicated by the loss of acetylenic protons. Specimens were collected at different times after exposure to air, purified, and then analyzed using both GPC and ^{1}H NMR. The ^{1}H NMR peaks (excluding the acetylene peak) of the coupled products were normalized to 1 and superimposed as shown in Figure 14.

The superimposed ^{1}H NMR spectra indicate a decrease over time in the acetylene peak (Ha) at around 2.45 ppm. The acetylene functionality was monitored for 24 h, after which the majority of the acetylene peak disappeared. The acetylene functionality was estimated by comparing the integration of Ha at different reaction times with the integration at t = 0. The

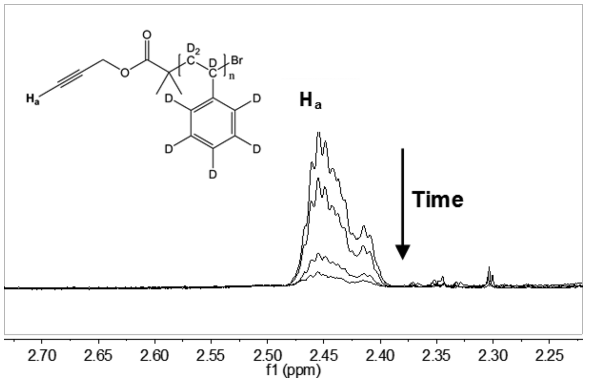

Figure 14. ^{1}H NMR (400 MHz) spectra recorded in $CDCl_3$ of deuterated α-alkyne,ω-Br-PS (Mn = 3090, PDI = 1.12) as a function of time after exposing the ATRP solution to air at room temperature.

reaction conversions calculated via ^{1}H NMR and GPC are shown in Table 1 as a function of exposure time to air.

Table 1. Comparison of Coupling Conversions between ^{1}H-NMR and GPC Studies

reaction time	^{1}H NMR conversion	GPC conversion
0	0	0
30	0.271	0.252
360	0.569	0.542
1440	0.866	0.868

Comparison of both values showed that the calculated conversions from the two methods were consistent with one another and clearly proves that the alkyne-terminated polymers underwent Glaser coupling post-ATRP, upon exposure to air.

Eliminating Glaser Coupling of Alkyne-Terminated Polymers by Maintaining Low Temperature after Polymerization during Copper Catalyst Removal. As shown in Figure 15, the Glaser coupling reaction post-ATRP can be completely suppressed by maintaining a low temperature (≤−28 °C) after polymerization. α-Alkyne,ω-Br-PS, was first synthesized via ATRP using neat styrene with PgBiB

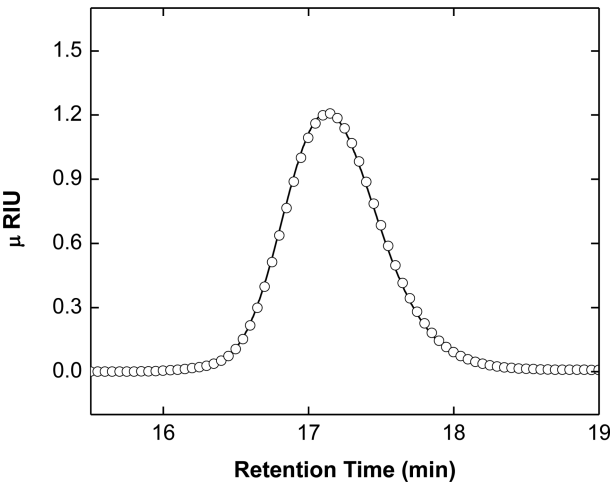

Figure 15. Superimposed GPC chromatograms of α-alkyne,ω-Br-PS (3310 g·mol^{-1}, PDI = 1.08) measured immediately after ATRP (—) and after a 16-h incubation exposed to air at −28 °C (○, plotted for every 30th data point).

DOI: 10.1021/jacs.6b12525
J. Am. Chem. Soc. 2017, 139, 3756−3766

initiator and CuBr/dNbpy catalyst ligand complex. Immediately after ATRP, the polymer samples were collected under inert atmosphere and analyzed via GPC. The samples were cooled and maintained at −28 °C, resulting in a dark green ATRP solution; the color indicating the presence of copper. The samples were then collected at different time intervals and purified (i.e., copper removed) by passing the solution through a cold neutral alumina column. Figure 15 shows GPC chromatograms collected immediately after ATRP (solid line) and after a 16-h incubation in air at ≤−28 °C (open circle). Figure S.4 superimposes GPC chromatograms of α-alkyne,ω-Br-P*t*BA, and α-alkyne,ω-Br-PS of higher molecular weights (Mn ≈ 10 000 g·mol^{-1}) before and after this incubation. In all cases, GPC signals superimpose perfectly indicating that the molecular weight distribution is unchanged after 16 h of incubation with air. Post-ATRP Glaser coupling is completely suppressed by maintaining low temperature after polymerization and during sample workup.

The suppression of Glaser coupling at low temperature can be ascribed to several factors. First, the decrease in temperature can affect the solubility of the catalyst/ligand complex and consequently the rate of Glaser Coupling. For α-alkyne,ω-Br-PS prepared by ATRP (Mn = 3170 g·mol^{-1}, PDI = 1.09) and subsequently exposed to air at different temperatures, the total solubility of copper as determined via ICP-OES decreased significantly from 1116 ppm at room temperature to 294 ppm at −28 °C. Huang and co-workers[65] reported similar findings for the CuBr/Bpy system, where a decrease in temperature from 110 to 70 °C caused a 5-fold decrease in the solubility of CuBr/Bpy in toluene and a 20-fold decrease for that of $CuBr_2$/Bpy in toluene. A decrease in temperature will also lower the rate of a polymer end-linking reaction because it will lower the rate of polymer diffusion. Vrentas and Duda,[66] for example, using Kirkwood-Riseman theories showed that the logarithm of the mutual-diffusion coefficient predicted for ethylbenzene-polystyrene system is inversely proportional to 1/*T*. Moreover, temperature may also affect the stability and concentration of the active copper/ligand complex species in the solution. For example, using temperature dependent Diffusion-Ordered NMR Spectroscopy, Gschwind and co-workers[67] were able to show a temperature-dependent interconversion of different phosphoramidite−Cu complex species in solution, directly affecting the activity of the compound. The combination of these factors could all play a role in suppressing Glaser coupling of alkyne end-functional polymers at low temperature.

Figure 16 presents GPC spectra measured immediately after low temperature copper removal by passing the ATRP solution through a cold alumina column and after a 16-h incubation with air in copper-free ATRP solution at room temperature. The two GPC signals superimpose perfectly showing identical molecular weight distributions and indicating the absence of any polymer coupling reactions. To corroborate the results, ^{1}H NMR was measured for PgBiB after a 24-h incubation with $CuBr_2$ and PMDETA. Comparison between the ^{1}H NMR spectra of pure PgBiB (Figure 8A) and after the 24-h incubation (Figure 8C) shows complete absence of both Glaser coupling and radical−radical coupling reactions. In contrast, a 24-h incubation of PgBib with CuBr and PMDETA resulted in the complete disappearance of the acetylene peak at δ = 2.51 ppm, indicating quantitative Glaser coupling of the alkyne groups. The results are consistent with works by Clifford and Water[68] and the Glaser coupling mechanisms proposed by

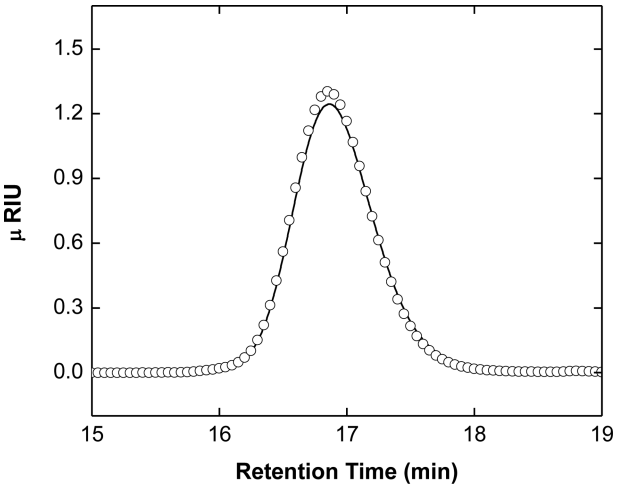

Figure 16. Superimposed GPC signals of α-alkyne,ω-Br-PS (3710 g·mol^{-1}, PDI = 1.10) taken immediately after copper removal (—) and after a 16-h incubation in copper-free solution (○, plotted for every 30th data point) at room temperature.

Bohlmann et al.[55] and Fomina et al.[57] that show that copper must be present for coupling to occur.

In summary, the results presented in Figures 15 and 16 demonstrate that ATRP using unprotected alkyne initiator is a viable means to prepare well-defined alkyne end-functional polymers provided that the temperature is kept below about −28 °C after polymerization and is followed by immediate copper removal using an alumina column held at low temperature. These conditions eliminate Glaser coupling.

Reducing Agents Eliminate RT Glaser Coupling of Alkynes under CuAAC Reaction Conditions. Figure 17 demonstrates that the addition of reducing agents eliminates Glaser coupling of alkyne molecules under CuAAC conditions. A small alkyne molecule, the initiator PgBiB, was incubated with $CuBr_2$, sodium L-ascorbate reducing agent, and PMDETA in THF and H_2O mixture and then exposed to air. Figure 17A presents the ^{1}H NMR spectrum of pure PgBiB and Figure 17B

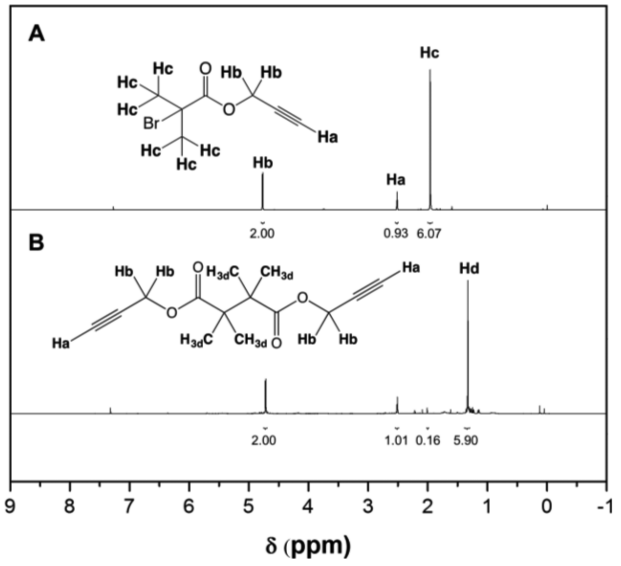

Figure 17. ^{1}H NMR (400 MHz) spectra recorded in $CDCl_3$ for (A) pure PgBiB and (B) a 24-h incubation of PgBiB with $CuBr_2$, sodium L-ascorbate, and PMDETA in THF and H_2O mixture.

DOI: 10.1021/jacs.6b12525
J. Am. Chem. Soc. 2017, 139, 3756−3766

shows the spectrum after the 24-h exposure to air. The relative peak area ratio between Hb at δ = 4.77 ppm and Ha at δ = 2.51 ppm remained constant at 2:1. The disappearance of the Hc peak at δ = 1.96 ppm and the appearance of the Hd peak at δ = 1.33 ppm, however indicate quantitative radical−radical coupling after prolonged incubation in excess Cu(I)/PMDETA to produce a dialkyne molecule. The ^{1}H NMR spectrum (Figure 17B) suggests that the ascorbate reducing agent, commonly used for CuAAC, was able to completely remove dissolved oxygen and prevent the oxidation of Cu(I) in the solution, thereby inhibiting Glaser coupling. It should be noted that, since this procedure resulted in a quantitative radical−radical coupling, it may constitute an effective future method for preparing telechelic dialkyne-functional molecules/macromolecules.

Reducing Agents Eliminate Room Temperature Glaser Coupling of Alkyne-Terminated Polymers Post ATRP. As demonstrated in Figure 18, the Glaser coupling reaction of alkyne polymers post-ATRP can be eliminated by the addition of reducing agents immediately after polymerization. The ATRP of styrene was performed with PgBiB initiator and CuBr/PMDETA catalyst−ligand complex. After polymerization, the ATRP product was added to a solution of excess $Sn(EH)_2$ reducing agent in toluene. After warming to room temperature, the solution was open to air and analyzed by GPC at various time intervals.

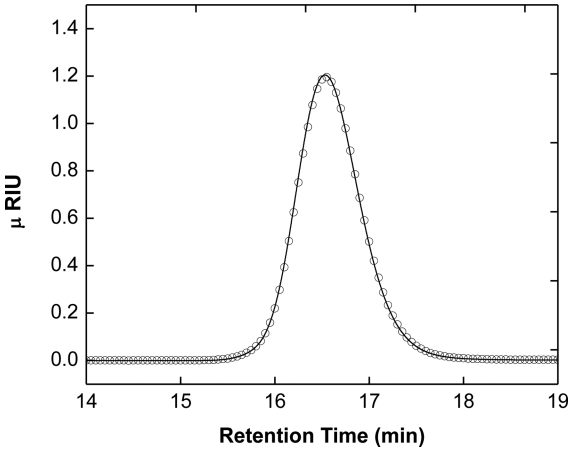

Figure 18. Superimposed GPC chromatograms of α-alkyne,ω-Br-PS (4450 g·mol^{-1}, PDI = 1.10) measured immediately after ATRP (—) and after a 20-h incubation open to air with $Sn(EH)_2$ (○, plotted for every 30th data point).

Figure 18 shows the superimposed GPC chromatograms of the α-alkyne,ω-Br-PS analyzed immediately after ATRP and after 20 h of exposure to air. The superimposed graphs, before and after the incubation, indicate identical molecular weight distributions centered at 16.6 min. Figure 18 clearly shows that the Glaser coupling reaction post-ATRP was completely suppressed by adding excess reducing agents after polymerization to prevent the formation of both Cu(II) and Cu(III) that are essential for the coupling reaction as indicated by the mechanisms proposed by Bohlmann et al.[55] and Fomine et al.,[57] respectively.

Reducing Agents Prevent Room Temperature Glaser Coupling during ARGET-ATRP Synthesis of Alkyne-Terminated Polymers in the Limited Presence of Air. Figure 19 shows the GPC spectra for α-alkyne,ω-Br-PS prepared by activators regenerated by electron transfer for atom transfer radical polymerization (ARGET-ATRP)[69] in the limited presence of air. The stacked GPC spectra show excellent control over the polymer's molecular weights and PDI. The distributions at lower conversions are monodispersed, indicating the absence of coupling reactions. Only at high conversion (>80%) was a bimodal molecular weight distribution observed, with the coupled product accounting to approximately 10% of the polymers produced. Matyjaszewski and co-workers reported that the formation of the bimodal distribution at high conversion was a result of radical coupling reactions as illustrated in Figure 1.[70] The high viscosity of the solution at high conversions significantly reduces the mobility of growing polymer chains and, consequently, the rate constant for deactivation. Thus, the rate of radical coupling accelerates, resulting in the polymer coupling reaction as evidenced by the bimodal distribution.

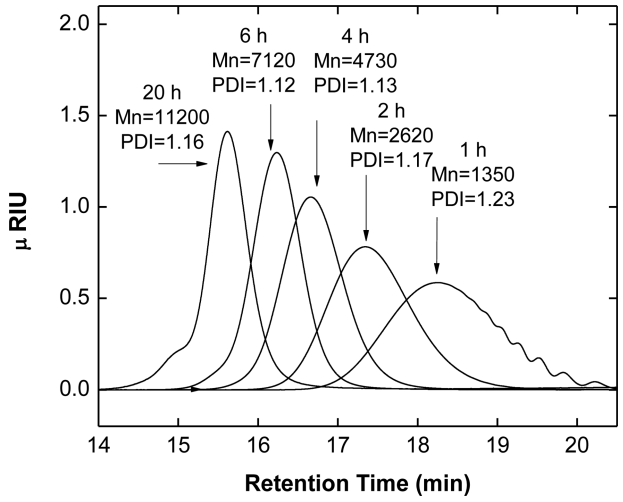

Figure 19. GPC signals during ARGET-ATRP of α-alkyne,ω-Br-PS.

Figure 20 demonstrates that the $Sn(EH)_2$ reducing agent used in the ARGET-ATRP procedure not only allows the polymerization to be performed in the presence of air, but also

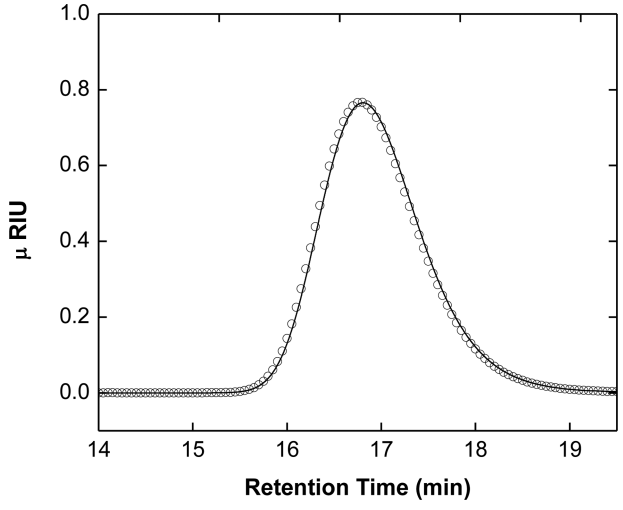

Figure 20. Superimposed GPC chromatograms of α-alkyne,ω-Br-PS (Mn = 3050, PDI = 1.22) measured immediately after ARGET ATRP (solid line) and after an 18-h incubation exposed to air at room temperature (○, plotted for every 30th data point).

DOI: 10.1021/jacs.6b12525
J. Am. Chem. Soc. 2017, 139, 3756−3766

effectively eliminates Glaser coupling. After 2.5 h of ARGET-ATRP, the reaction solution was cooled to room temperature and the reaction vial was opened to air. Figure 20 shows the superimposed GPC chromatograms of α-alkyne,ω-Br-PS analyzed immediately after ARGET-ATRP and after an 18-h incubation. The superimposed graphs, before and after the incubation, show an unchanged molecular weight distributions centered at 16.9 min. While ARGET-ATRP does eliminate Glaser coupling, it unfortunately produces a polymer with a broader molecular weight distribution (PDI = 1.22) than that synthesized by normal ATRP (PDI = 1.09), due to the limited presence of oxygen and the reduction in the number of Cu(II) deactivator species by the addition of $Sn(EH)_2$ during ARGET-ATRP, affecting the rate of chain deactivation. Nevertheless, by lowering the concentration of the copper catalyst to 50 ppm, we were able to effectively control the rate of the polymerization process. Moreover, Matyjaszewski and co-workers reported that lowering the catalyst concentration also reduces other catalyst-induced side reactions in ARGET ATRP such as the β-H elimination of the bromine terminus which affects the bromine functionality of the synthesized polymers.[70]

In short summary, the results presented in Figures 17−20 demonstrate that Glaser coupling associated with the ATRP of alkyne functional molecules/macromolecules can be eliminated simply by the addition of mild reducing agents such as tin(II) 2-ethylhexanoate or (+)-sodium L-ascorbate. We also show that Glaser coupling does not occur during or after ARGET-ATRP due to the presence of reducing agent during polymerization.

Effect of ATRP Synthesis Ligands on Glaser Coupling of Alkyne-Terminated Polymers. The influence of various nitrogen-based ATRP synthesis ligands (see Figure 21) on the post-ATRP Glaser coupling of α-alkyne,ω-Br-PS was evaluated by GPC analysis. For comparison sake, attempts were made in these experiments to achieve a final molecular weight of ~3000 g·mol^{-1} (Mn) for the α-alkyne,ω-Br-PS. The results in Figure 22 show that linear bidentate ligands (dNbpy and dBbpy) were significantly more active than a tridentate ligand (PMDETA), which in turn were more active than a tetradentate ligand (HMTETA) in catalyzing the Glaser coupling reaction. The results are consistent with previous reports by Hay and co-workers,[48] who first performed oxidative acetylenic coupling in the presence of bidentate ligand, *N*,*N*,*N*′,*N*′-tetramethylethylenediamine (TMEDA) and Cu(I)Cl. While TMEDA has been accepted as the "model" ligand for acetylene coupling of small alkyne molecules, when used for ATRP, it produces polymers with high PDIs (>1.4) due to the high reactivity of the Cu(I)/TMEDA complex; therefore, TMEDA was not investigated in this study.

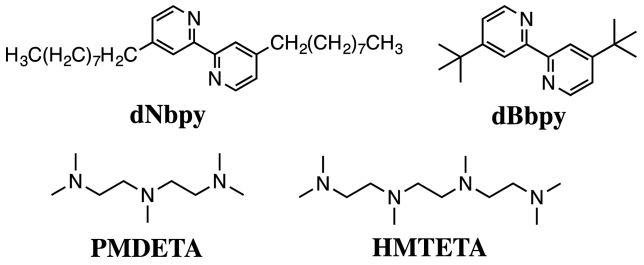

Figure 21. Structures of ATRP ligands used for Glaser coupling studies.

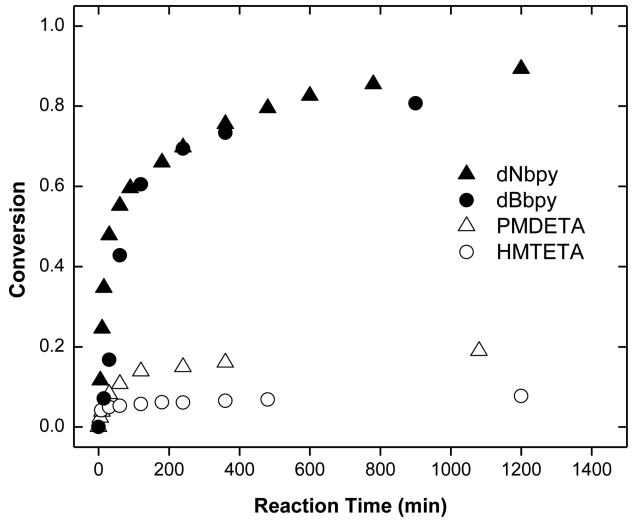

Figure 22. Coupling conversion of α-alkyne,ω-Br-PS (▲ Mn = 2930 g·mol^{-1}, PDI = 1.09; ● Mn = 2680 g·mol^{-1}, PDI = 1.10; ΔMn = 3390 g·mol^{-1}, PDI = 1.11; ○ Mn = 3300 g·mol^{-1}, PDI = 1.17) with different ATRP ligands as a function of time.

Higher ligand denticity can reduce the Glaser Coupling rates by coordinatively saturating the Cu(I) catalyst and hindering coordination to the alkyne, which is the essential reaction step as shown in both Glaser Coupling mechanisms in Figure 2 and 3. Interestingly, ligand denticity has also been shown to affect the CuAAC reaction rates of alkynes and azides.[71] Tetradentate ligands were reported to produce lower CuAAC reaction rates compared to tridentate and bidentate ligands. In both the CuAAC and Glaser Coupling mechanisms, the Cu(I) catalyst is involved in the formation of Cu(I)-alkyne π-complexation.[72,73] Therefore, the use of higher ligand denticity (i.e., tetradentate ligands) may interfere with the formation of the complex, and thus decrease the rate of the coupling reactions. In summary, results in Figure 22 show that appropriate choice of a nitrogen-based ATRP ligand can significantly reduce but not eliminate Glaser coupling.

■ CONCLUSIONS

Alkyne-alkyne (i.e., Glaser) coupling is a side reaction that adversely affects the fidelity of both the synthesis of alkyne-functional polymers (i.e., by ATRP) and click reactions of alkynes (i.e., CuAAC). ^{1}H NMR and GPC experiments demonstrate that Glaser coupling does not occur during ATRP of alkyne-functional polymers, when air is absent, but upon exposure to air post-ATRP during sample workup. Upon exposure to air, XPS experiments show that some of the Cu(I) present under ATRP conditions is oxidized in situ to generate the Cu(II) required to catalyze the Glaser coupling reaction. We introduce two new strategies for the elimination of Glaser coupling associated with the ATRP of alkyne-terminated polymers and for alkynes under CuAAC reaction conditions. First, by maintaining low temperature post-ATRP followed by immediate low-temperature copper catalyst removal, the Glaser coupling reaction was completely suppressed; alkyne-terminated polymers of high-functionality were produced without the need for alkyne protecting groups. Second, the use of excess reducing agents, such as tin(II) 2-ethylhexanoate or (+)-sodium L-ascorbate, eliminated Glaser coupling associated with ATRP and ARGET ATRP synthesis of alkyne-functional polymers, as well as for alkynes held under CuAAC reaction conditions.

DOI: 10.1021/jacs.6b12525
J. Am. Chem. Soc. 2017, 139, 3756−3766

Glaser coupling associated with the ATRP synthesis of alkyne-functional polymers is also influenced by the nitrogen-based ligand used. Linear bidentate ligands (dNbpy and dBbpy) were significantly more active than tridentate (PMDETA), which in turn were more active than tetradentate ligands (HMTETA) in catalyzing the Glaser coupling reaction.

■ ASSOCIATED CONTENT

Supporting Information

The Supporting Information is available free of charge on the ACS Publications website at DOI: 10.1021/jacs.6b12525.

All experimental procedures and experimental polymerization conditions. GPC and ^{1}H NMR data of Glaser Coupling reactions (or lack of) for nonfunctional PS, α-alkyne,ω-Br-PS and α-alkyne,ω-Br-P*t*BA with varying molecular weights.(PDF)

■ AUTHOR INFORMATION

Corresponding Author

*jk1191@columbia.edu

ORCID

Jeffrey T. Koberstein: 0000-0002-7946-3125

Author Contributions

All authors have given approval to the final version of the manuscript.

Notes

The authors declare no competing financial interest.

■ ACKNOWLEDGMENTS

The research was supported by the US Army Research Office (Grants W911NF1010184 and W911NF1110372) and by the National Science Foundation (Grant DMR1206191 from the Polymers Program). We would also like to acknowledge Djordje Vuckovic at Columbia University for his help with background literature surveys and Glaser kinetics studies.

■ REFERENCES

(1) Kolb, H. C.; Sharpless, K. B. *Drug Discovery Today* **2003**, *8*, 1128−1137.
(2) Tron, G. C.; Pirali, T.; Billington, R. A.; Canonico, P. L.; Sorba, G.; Genazzani, A. A. *Med. Res. Rev.* **2008**, *28*, 278−308.
(3) Sletten, E. M.; Bertozzi, C. R. *Angew. Chem., Int. Ed.* **2009**, *48*, 6974−6998.
(4) Jung, S.; Yi, H. *Langmuir* **2012**, *28*, 17061−17070.
(5) Gil, M.; Arévalo, M.; López, Ó. *Synthesis* **2007**, *2007*, 1589−1620.
(6) Binder, W. H.; Kluger, C. *Curr. Org. Chem.* **2006**, *10*, 1791−1815.
(7) Wu, P.; Feldman, A. K.; Nugent, A. K.; Hawker, C. J.; Scheel, A.; Voit, B.; Pyun, J.; Fréchet, J. M. J.; Sharpless, K. B.; Fokin, V. V. *Angew. Chem., Int. Ed.* **2004**, *43*, 3928−3932.
(8) Binder, W. H.; Sachsenhofer, R. *Macromol. Rapid Commun.* **2007**, *28*, 15−54.
(9) Tunca, U. *J. Polym. Sci., Part A: Polym. Chem.* **2014**, *52*, 3147−3165.
(10) Mansfeld, U.; Pietsch, C.; Hoogenboom, R.; Becer, C. R.; Schubert, U. S. *Polym. Chem.* **2010**, *1*, 1560.
(11) Lutz, J.-F. *Angew. Chem., Int. Ed.* **2007**, *46*, 1018−1025.
(12) Fournier, D.; Hoogenboom, R.; Schubert, U. S. *Chem. Soc. Rev.* **2007**, *36*, 1369.
(13) Helms, B.; Mynar, J. L.; Hawker, C. J.; Fréchet, J. M. J. *J. Am. Chem. Soc.* **2004**, *126*, 15020−15021.
(14) Dedola, S.; Nepogodiev, S. a; Field, R. a. *Org. Biomol. Chem.* **2007**, *5*, 1006−1017.
(15) Spain, S. G.; Gibson, M. I.; Cameron, N. R. *J. Polym. Sci., Part A: Polym. Chem.* **2007**, *45*, 2059−2072.
(16) Baskin, J. M.; Prescher, J. A.; Laughlin, S. T.; Agard, N. J.; Chang, P. V.; Miller, I. A.; Lo, A.; Codelli, J. A.; Bertozzi, C. R. *Proc. Natl. Acad. Sci. U. S. A.* **2007**, *104*, 16793−16797.
(17) Speers, A. E.; Cravatt, B. F. *Chem. Biol.* **2004**, *11*, 535−546.
(18) Chen, L.; Rengifo, H. R.; Grigoras, C.; Li, X.; Li, Z.; Ju, J.; Koberstein, J. T. *Biomacromolecules* **2008**, *9*, 2345−2352.
(19) Zhang, S.; Maidenberg, Y.; Luo, K.; Koberstein, J. T. *Langmuir* **2014**, *30*, 6071−6078.
(20) Maidenberg, Y.; Zhang, S.; Luo, K.; Akhavein, N.; Koberstein, J. T. *Langmuir* **2013**, *29*, 11959−11965.
(21) White, M. A.; Johnson, J. a; Koberstein, J. T.; Turro, N. J. *J. Am. Chem. Soc.* **2006**, *128*, 11356−11357.
(22) Ranjan, R.; Brittain, W. J. *Macromolecules* **2007**, *40*, 6217−6223.
(23) Chen, G.; Tao, L.; Mantovani, G.; Ladmiral, V.; Burt, D. P.; Macpherson, J. V.; Haddleton, D. M. *Soft Matter* **2007**, *3*, 732−739.
(24) Kolb, H. C.; Finn, M. G.; Sharpless, K. B. *Angew. Chem., Int. Ed.* **2001**, *40*, 2004−2021.
(25) Rostovtsev, V. V.; Green, L. G.; Fokin, V. V.; Sharpless, K. B. *Angew. Chem., Int. Ed.* **2002**, *41*, 2596−2599.
(26) Tsarevsky, N. V.; Sumerlin, B. S.; Matyjaszewski, K. *Macromolecules* **2005**, *38*, 3558−3561.
(27) Johnson, J. A.; Lewis, D. R.; Díaz, D. D.; Finn, M. G.; Koberstein, J. T.; Turro, N. J. *J. Am. Chem. Soc.* **2006**, *128*, 6564−6565.
(28) Johnson, J. A.; Finn, M. G.; Koberstein, J. T.; Turro, N. J. *Macromolecules* **2007**, *40*, 3589−3598.
(29) Johnson, J. A.; Finn, M. G.; Koberstein, J. T.; Turro, N. J. *Macromol. Rapid Commun.* **2008**, *29*, 1052−1072.
(30) Opsteen, J. A.; Van Hest, J. *J. Polym. Sci., Part A: Polym. Chem.* **2007**, *45*, 2913−2924.
(31) Van Camp, W.; Germonpré, V.; Mespouille, L.; Dubois, P.; Goethals, E. J.; Du Prez, F. E. *React. Funct. Polym.* **2007**, *67*, 1168−1180.
(32) Liu, Q.; Zhao, P.; Chen, Y. *J. Polym. Sci., Part A: Polym. Chem.* **2007**, *45*, 3330−3341.
(33) Laurent, B. A.; Grayson, S. M. *J. Am. Chem. Soc.* **2006**, *128*, 4238−4239.
(34) Bunha, A.; Cao, P.-F.; Mangadlao, J.; Shi, F.-M.; Foster, E.; Pangilinan, K.; Advincula, R. *Chem. Commun.* **2015**, *51*, 7528−7531.
(35) Deng, G.; Ma, D.; Xu, Z. *Eur. Polym. J.* **2007**, *43*, 1179−1187.
(36) Gao, H.; Matyjaszewski, K. *Macromolecules* **2006**, *39*, 4960−4965.
(37) Durmaz, H.; Dag, A.; Gursoy, D.; Demirel, A. L.; Hizal, G.; Tunca, U. *J. Polym. Sci., Part A: Polym. Chem.* **2010**, *48*, 1557−1564.
(38) Rengifo, H. R.; Grigoras, C.; Dach, B. I.; Li, X.; Turro, N. J.; Lee, H.-J.; Wu, W.-L.; Koberstein, J. T. *Macromolecules* **2012**, *45*, 3866−3873.
(39) Wang, J.-S.; Matyjaszewski, K. *J. Am. Chem. Soc.* **1995**, *117*, 5614−5615.
(40) Matyjaszewski, K.; Xia, J. *Chem. Rev.* **2001**, *101*, 2921−2990.
(41) Lin, W.; Fu, Q.; Zhang, Y.; Huang, J. *Macromolecules* **2008**, *41*, 4127−4135.
(42) Golas, P. L.; Tsarevsky, A. N. V; Sumerlin, A. B. S.; Walker, L. M.; Matyjaszewski, K. *Aust. J. Chem.* **2007**, *60* (60), 400−404.
(43) Cheng, C.; Bai, X.; Zhang, X.; Chen, M.; Huang, Q.; Hu, Z.; Tu, Y. *Macromol. Res.* **2014**, *22*, 1306−1311.
(44) Rocha, N.; Mendonça, P. V.; Mendes, J. P.; Simões, P. N.; Popov, A. V.; Guliashvili, T.; Serra, A. C.; Coelho, J. F. J. *Macromol. Chem. Phys.* **2013**, *214*, 76−84.
(45) Hou, C.; Lin, S.; Liu, F.; Hu, J.; Zhang, G.; Liu, G.; Tu, Y.; Zou, H.; Luo, H. *New J. Chem.* **2014**, *38*, 2538.
(46) Duxbury, C. J.; Cummins, D.; Heise, A. *J. Polym. Sci., Part A: Polym. Chem.* **2009**, *47*, 3795−3802.
(47) Tornøe, C. W.; Christensen, C.; Meldal, M. *J. Org. Chem.* **2002**, *67*, 3057−3064.
(48) Hay, A. S. *J. Org. Chem.* **1962**, *27*, 3320−3321.
(49) Siemsen, P.; Livingston, R. C.; Diederich, F. *Angew. Chem., Int. Ed.* **2000**, *39* (15), 2632−2657.
(50) Tour, J. M. *Chem. Rev.* **1996**, *96*, 537−554.
(51) Eppel, S.; Portnoy, M. *Tetrahedron Lett.* **2013**, *54*, 5056−5060.

DOI: 10.1021/jacs.6b12525
J. Am. Chem. Soc. 2017, 139, 3756−3766

(52) Anthony, J.; Boudon, C.; Diederich, F.; Gisselbrecht, J.-P.; Gramlich, V.; Gross, M.; Hobi, M.; Seiler, P. *Angew. Chem., Int. Ed. Engl.* **1994**, *33*, 763−766.
(53) Wang, G.; Hu, B.; Fan, X.; Zhang, Y.; Huang, J. *J. Polym. Sci., Part A: Polym. Chem.* **2012**, *50*, 2227−2235.
(54) Zhang, Y.; Wang, G.; Huang, J. *Macromolecules* **2010**, *43*, 10343−10347.
(55) Bohlmann, F.; Schönowsky, H.; Inhoffen, E.; Grau, G. *Chem. Ber.* **1964**, *97*, 794−800.
(56) Jover, J.; Spuhler, P.; Zhao, L.; McArdle, C.; Maseras, F. *Catal. Sci. Technol.* **2014**, *4*, 4200−4209.
(57) Fomina, L.; Vazquez, B.; Tkatchouk, E.; Fomine, S. *Tetrahedron* **2002**, *58*, 6741−6747.
(58) Elupula, R.; Oh, J.; Haque, F. M.; Chang, T.; Grayson, S. M. *Macromolecules* **2016**, *49*, 4369−4372.
(59) Sreerama, S. G.; Elupula, R.; Laurent, B. A.; Zhang, B.; Grayson, S. M. *React. Funct. Polym.* **2014**, *80*, 83−94.
(60) Meldal, M.; Tornøe, C. W. *Chem. Rev.* **2008**, *108*, 2952−3015.
(61) Angell, Y.; Burgess, K. *Angew. Chem., Int. Ed.* **2007**, *46*, 3649−3651.
(62) Himo, F.; Lovell, T.; Hilgraf, R.; Rostovtsev, V. V.; Noodleman, L.; Sharpless, K. B.; Fokin, V. V. *J. Am. Chem. Soc.* **2005**, *127*, 210−216.
(63) Barner-Kowollik, C. *Macromol. Rapid Commun.* **2009**, *30*, 1625−1631.
(64) Friedman, B.; O'Shaughnessy, B. *Macromolecules* **1993**, *26*, 5726−5739.
(65) Chen, Z.-C.; Chiu, C.-L.; Huang, C.-F. *Polymers (Basel, Switz.)* **2014**, *6*, 2552−2572.
(66) Vrentas, J. S.; Duda, J. L. *J. Polym. Sci., Polym. Phys. Ed.* **1977**, *15*, 417−439.
(67) Schober, K.; Zhang, H.; Gschwind, R. M. *J. Am. Chem. Soc.* **2008**, *130*, 12310−12317.
(68) Clifford, A. A.; Waters, W. A. *J. Chem. Soc.* **1963**, 3056.
(69) Jakubowski, W.; Min, K.; Matyjaszewski, K. *Macromolecules* **2006**, *39*, 39−45.
(70) Jakubowski, W.; Kirci-Denizli, B.; Gil, R. R.; Matyjaszewski, K. *Macromol. Chem. Phys.* **2008**, *209*, 32−39.
(71) Golas, P. L.; Tsarevsky, N. V.; Sumerlin, B. S.; Matyjaszewski, K. *Macromolecules* **2006**, *39*, 6451−6457.
(72) Rodionov, V. O.; Fokin, V. V.; Finn, M. G. *Angew. Chem., Int. Ed.* **2005**, *44*, 2210−2215.
(73) Bock, V. D.; Hiemstra, H.; van Maarseveen, J. H. *Eur. J. Org. Chem.* **2006**, *2006*, 51−68.

DOI: 10.1021/jacs.6b12525
J. Am. Chem. Soc. 2017, 139, 3756−3766